J. Earth Planet. Sci. Nagoya Univ., Vol. 43, 17 to 26, 1996

CHIME dating of monazite from pelitic hornfels of the Kurihashi Granodiorite, Kitakami Mountains

Kazuhiro SUZUKI*, Hidekazu YOSHIDA, Kenji AMANO*** and Setsuo YOGO***

**Department of Earth and Planetary Sciences, Nagoya University, Nagoya 464-01, Japan*
***Power Reactor and Nuclear Fuel Development Corporation, Tono Geoscience Center, Jorinji, Toki 509-51, Japan*
****Power Reactor and Nuclear Fuel Development Corporation, Kamaishi Site Office, Kassi, Kamaishi 026, Japan*
(Received September 24, 1996 / Accepted November 1, 1996)

ABSTRACT

The Cretaceous Kurihashi Granodiorite in the Kitakami Mountains contains no monazite grain. To date the emplacement time of the Kurihashi Granodiorite by the CHIME method, monazite in a hornfels from the immediate contact of the granodiorite, instead, was analyzed. A total of 159 analyses on 17 monazite grains define an isochron of 117.7 ± 2.0 Ma with an intercept value of 0.0005 ± 0.0005. This age can be interpreted as the time of monazite formation during the contact metamorphism due to the emplacement of the Kurihashi Granodiorite.

INTRODUCTION

The usual objective of dating granitoids is to know their ages of emplacement or crystallization. Some problems associated with dating a suite of young granitoids include (1) the presence of crustal contamination and inheritance, (2) the absence of compositional variation required for the isochron method, (3) the inter-pluton thermal overprints, and (4) the intense weathering and/or alteration. Geochronological work in recent years has shown that monazite in granitoids dates the time of crystallization, because of its high blocking temperature for Pb (Schärer et al., 1984; Suzuki et al., 1994, 1996; Nakai and Suzuki, 1996). This mineral, with a high concentration of Th and U, has the ability to accumulate an amount of Pb sufficient for precise electron microprobe analyses within 50–100 m.y. of its formation, and is suitable for the CHIME dating.

Monazite, however, is uncommon in granitoids of somewhat basic compositions like granodiorite or diorite. We searched for an alternative way to date monazite-free granitoids by the CHIME method, and found that most pelitic hornfels from the immediate contact of granitoids contain sizable grains of monazite. These monazite grains are interpreted to be formed during the

contact metamorphism; the monazite age is likely to show the emplacement time of granitoids. We report here the result of CHIME dating of monazite from a pelitic hornfels in contact with the Cretaceous Kurihashi Granodiorite in the Kitakami Mountains, Northeast Japan. This may provide crucial information on how to date monazite-free granitoids by the CHIME method.

GEOLOGY AND SAMPLE DESCRIPTION

The geological configuration of the sampling site is illustrated in Fig. 1. The Kamaishi Mine, now closed and one of the major copper-iron mines of the

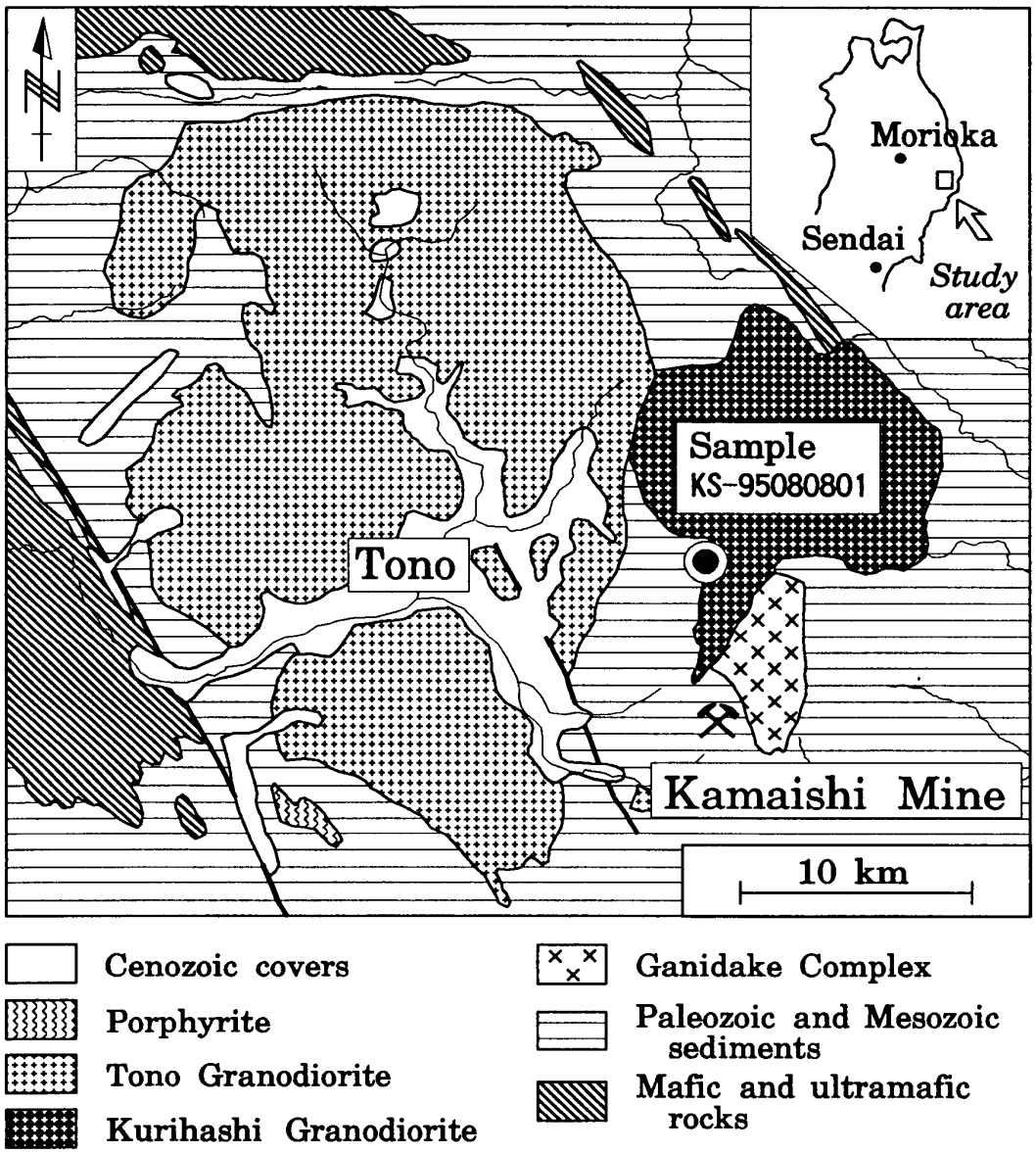

Fig. 1. Geologic configuration of the Kurihashi Granodiorite and related granitoids in the Kitakami Mountains (modified and simplified from Owa, 1956, Hamabe and Yano, 1976, Yamazaki et al., 1983 and Yoshida et al., 1984).

skarn-type in Japan, is located in the southeastern part of the map area. The area is underlain mainly by Paleozoic and Mesozoic sedimentary rocks and Cretaceous granitoids (Owa, 1956; Hamabe and Yano, 1976; Yamazaki et al., 1983; Yoshida et al., 1984). Granitoids include the Ganidake Complex, the Kurihashi Granodiorite and the Tono Granodiorite. The Ganidake Complex crops out over a NNW-SSE elongated area of 4.5×2 km, and consists of diorite porphyry, diorite, granodiorite and monzonite. This complex is considered to have played an important role on the formation of ore bodies in the Kamaishi Mine (Hamabe and Yano, 1976). The Kurihashi Granodiorite crops out over an area of 15×11 km and forms a basin structure (Kano et al. 1978). The Tono Granodiorite covers an area of 40×20 km, showing a dome structure with subordinate basins in western and southern margins (Kano et al. 1978). Hamabe and Yano (1976) described that the Kurihashi Granodiorite is geologically younger than the Ganidake Complex. However, the intrusive relation between the Kurihashi and Tono Granodiorites is still unclear owing to no appropriate exposure.

The Kurihashi Granodiorite is medium- to coarse-grained, and is composed mainly of plagioclase, quartz, K-feldspar, hornblende and biotite, with accessories of zircon, apatite, magnetite, titanite, and ilmenite. Hornblende is pale brownish green in color. Biotite is dark brown and is replaced by chlorite and prehnite along the cleavage.

The hornfels sample (No. KS-95080801) was collected from the immediate contact with the Kurihashi Granodiorite (Fig. 1: 141°40′25″E, 39°20′42″N). It is a pelitic hornfels, and consists mainly of quartz, plagioclase, K-feldspar, biotite and cordierite. Accessory minerals include monazite, zircon, tourmaline and apatite. This sample does not contain muscovite that is common in pelitic and psammitic hornfels apart more than 100 m from the contact; the cordierite plus K-feldspar assemblage is estimated to have formed by the decomposition of muscovite under the presence of biotite and quartz. Since the metamorphic grade increases toward the Kurihashi Granodiorite, the mineral assemblage of the sample has formed by the thermal effect of the Kurihashi Granodiorite, not by the Ganidake Complex and the Tono Granodiorite. Monazite grains disperse between and within main constituent minerals of the sample (Figs. 2a and 2b), but in muscovite-bearing samples it is rare and small in size. This suggests that monazite grains in sample KS-95080801 crystallized during the contact metamorphism of the Kurihashi Granodiorite.

CHIME MONAZITE AGE

Monazite grains were separated from about 2 kg of the powdered (<80 mesh) sample by panning. They form subhedral to anhedral grains of about 0.05—0.1 mm in size (Figs. 2c and 2d). The ThO_2, UO_2 and PbO contents of monazite were analyzed on a JXA-733 electron microprobe. Experimental details including the analytical procedure and CHIME age calculation were reported elsewhere (e.g. Suzuki et al., 1991, 1994; Suzuki and Adachi, 1991a,b,

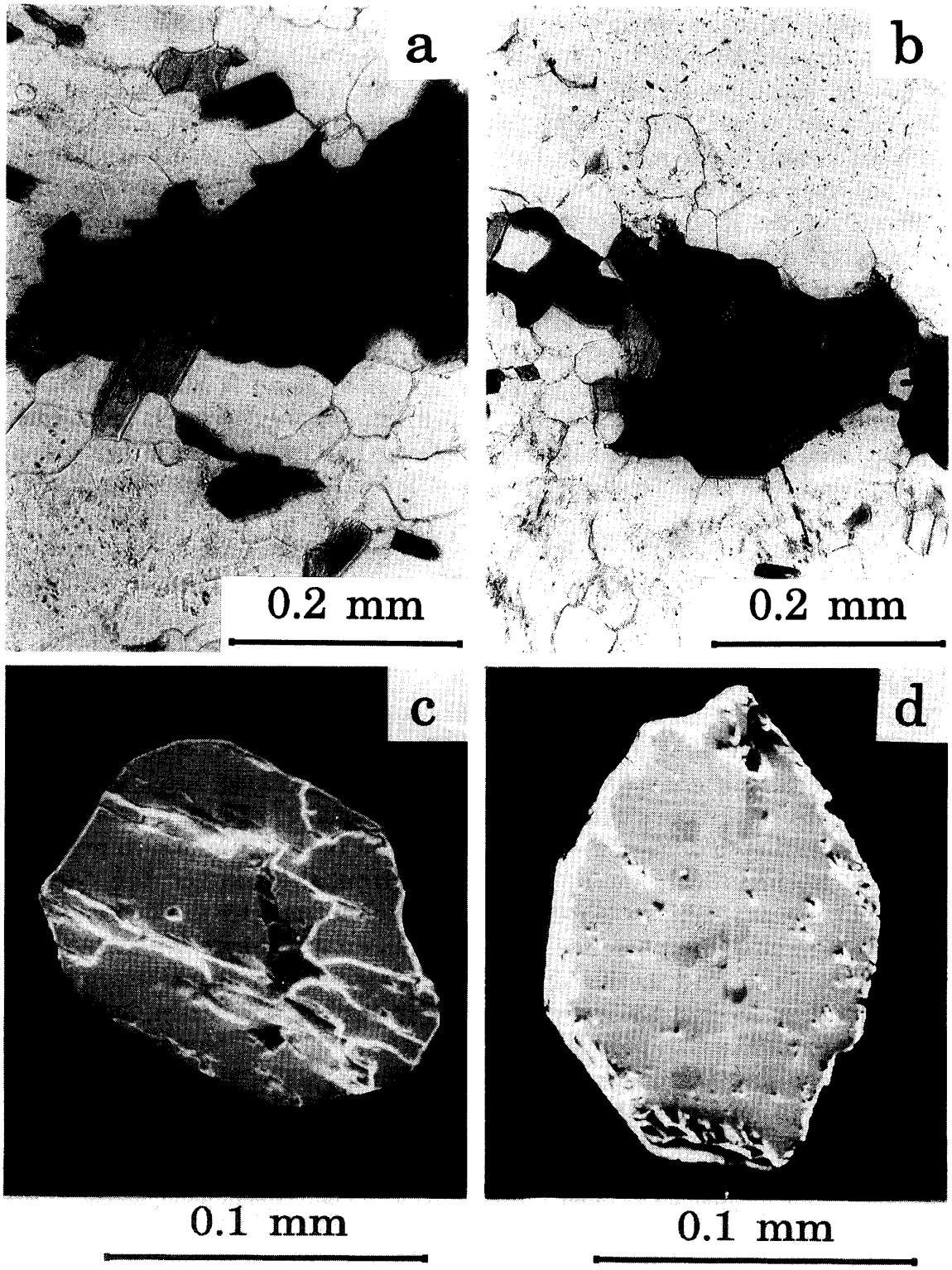

Fig. 2. Photomicrographs of monazite (central portions of a and b) and zircon (upper left of b) contained in aggregates of biotite flakes in sample KS-95080801. Note that the pleochroic haloes (dark ring) around monazite is much more prominent than those around zircon. Photomicrographs of back scattered electron images of M09 (c) and M17 (d) monazite grains. The analyzed area are visible as small circular dark spots.

1994; Adachi and Suzuki, 1992). Microprobe analyses of ThO_2, UO_2 and PbO are given in Table 1, together with the ThO_2* value (measured ThO_2 plus the ThO_2 equivalent of the measured UO_2) and apparent age. The detection limits of PbO at 2σ confidence level are 0.006 wt.%, and the relative error is about 10—15% for 0.02 wt.% of the PbO concentration.

A total of 159 spots on 17 monazite grains were analyzed. The ThO_2 concentration ranges from 2.41 to 15.0%, the UO_2 concentration from 0.054 to 1.14%, the PbO concentration from 0.0138 to 0.0787%, and the U/Th atomic ratio from 0.012 to 0.178 (Table 1). Analytical data are plotted on the PbO vs. ThO_2* diagram (Fig. 3). All the data points are arrayed linearly on the diagram, and give a well-defined isochron of 117.7 ± 2.0 Ma (MSWD = 0.10) with an intercept value of 0.0005 ± 0.0005. No signature of older ages can be seen on any part of individual monazite grains.

DISCUSSION

As noted above, the CHIME monazite age for the hornfels sample is 117.7 ± 2.0 Ma. Before accepting this CHIME monazite age as that for the emplacement of the Kurihashi Granodiorite, an alternative interpretation needs to be examined. Some may consider that monazite in the hornfels is newly formed as a result of a process other than the contact metamorphism. This process may include crystallization of monazite from a non-metamorphic, REE-rich fluid as envisaged by Corfu and Muir (1989). In sample KS-95080801, monazite disperses as 0.05—0.1 mm grains between and within main constituent minerals, and does not occur in veins or microcracks as might be expected of a mineral crystallized during fluid infiltration. Furthermore, we have not observed any REE minerals likely co-precipitating from such fluids. We also note the preservation of the high-grade metamorphic assemblage of cordierite-biotite-K-feldspar-plagioclase-quartz without any retrograde and hydrothermal modification. These lines of petrographic evidence do not support crystallization of monazite from a non-metamorphic REE-rich fluid.

Sawka et al. (1986) speculated that monazite in metasediments (precursors of S-type granites) crystallizes through dehydration of REE-rich hydrous phosphates. Smith and Barreiro (1990) found that the monazite-forming reaction takes place at lower amphibolite facies conditions, and that the Th-U-Pb system records the time since the formation. Monazite is likely to have formed as a metamorphic mineral during the contact metamorphism. Thus, the monazite age dates directly the emplacement of the Kurihashi Granodiorite.

The Kurihashi Granodiorite, the Ganidake Complex and the Tono Granodiorite have been dated by Kawano and Ueda (1965) through the K-Ar method; the K-Ar biotite ages are 120, 120 and 122 Ma for the Kurihashi Granodiorite, 119 Ma for the Ganidake Complex, and 110, 114, 114, 119, 119, 120 and 122 Ma for the Tono Granodiorite (errors in ages are not referred in the article). Shibata (1974) reported Rb-Sr whole-rock isotopic data for 4 samples

Table 1. Microprobe analyses of ThO_2, UO_2 and PbO of monazites from hornfels sample KS-95080801 in contact with the Kurihashi Granodiorite in the Kitakami Mountains.

Grain No.	ThO_2 (wt%)	UO_2 (wt%)	PbO (wt%)	Age (Ma)	ThO_2* (wt%)	Grain No.	ThO_2 (wt%)	UO_2 (wt%)	PbO (wt%)	Age (Ma)	ThO_2* (wt%)
M01-01	6.90	0.165	0.0365	116	7.43	M03-10	8.85	0.138	0.0473	120	9.29
M01-02	7.50	0.217	0.0398	115	8.20	M03-11	4.88	0.074	0.0266	123	5.12
M01-03	6.92	0.357	0.0408	120	8.07	M03-12	7.09	0.100	0.0378	121	7.41
M01-04	6.46	0.762	0.0454	121	8.91	M03-13	5.72	0.090	0.0292	115	6.01
M01-05	6.63	0.735	0.0439	116	8.99	M04-01	6.51	0.175	0.0352	118	7.07
M01-06	6.80	0.620	0.0451	121	8.79	M04-02	9.88	0.108	0.0512	118	10.2
M01-07	6.35	1.03	0.0492	121	9.66	M04-03	6.28	0.144	0.0331	116	6.74
M01-08	6.78	0.469	0.0395	113	8.29	M04-04	9.46	0.255	0.0513	118	10.3
M01-09	6.85	0.477	0.0440	124	8.38	M04-05	6.32	0.134	0.0333	117	6.75
M01-10	6.01	0.076	0.0290	110	6.25	M04-06	5.97	0.111	0.0333	124	6.33
M01-11	6.45	0.526	0.0393	114	8.14	M04-07	3.77	0.108	0.0206	118	4.12
M01-12	6.63	0.715	0.0471	125	8.93	M04-08	2.79	0.076	0.0157	122	3.03
M01-13	6.54	0.633	0.0419	116	8.57	M04-09	6.00	0.344	0.0350	117	7.10
M01-14	5.75	0.594	0.0386	119	7.66	M04-10	7.14	0.396	0.0409	115	8.41
M01-15	5.72	0.599	0.0402	124	7.64	M04-11	7.15	0.416	0.0431	120	8.49
M01-16	6.25	0.649	0.0434	123	8.33	M04-12	6.63	0.375	0.0381	115	7.83
M01-17	6.28	0.612	0.0410	118	8.25	M04-13	6.18	0.135	0.0347	124	6.61
M01-18	6.22	0.487	0.0394	120	7.78	M04-14	5.60	0.131	0.0313	123	6.02
M01-19	6.05	0.984	0.0471	121	9.21	M04-15	5.07	0.109	0.0256	112	5.42
M01-20	6.24	1.04	0.0470	116	9.58	M04-16	8.50	0.246	0.0479	122	9.29
M01-21	5.68	0.609	0.0386	119	7.64	M04-17	8.61	0.094	0.0455	121	8.91
M01-22	5.80	0.564	0.0371	115	7.61	M05-01	3.80	0.061	0.0212	126	4.00
M02-01	5.01	0.079	0.0266	120	5.26	M05-02	4.24	0.054	0.0222	119	4.41
M02-02	7.62	0.138	0.0402	118	8.06	M05-03	4.14	0.064	0.0234	128	4.34
M02-03	8.78	0.136	0.0476	122	9.22	M05-04	4.71	0.068	0.0262	126	4.93
M02-04	5.11	0.097	0.0283	123	5.42	M05-05	4.08	0.061	0.0225	125	4.28
M02-05	6.18	0.082	0.0319	117	6.44	M05-06	6.14	0.061	0.0305	114	6.33
M02-06	7.54	0.131	0.0426	126	7.96	M06-01	3.69	0.204	0.0222	121	4.34
M02-07	6.59	0.088	0.0350	120	6.87	M06-02	4.73	0.206	0.0260	114	5.39
M02-08	8.19	0.112	0.0431	119	8.55	M06-03	3.52	0.223	0.0210	117	4.24
M02-09	8.02	0.136	0.0423	118	8.46	M07-01	2.75	0.181	0.0162	115	3.33
M03-01	6.29	0.092	0.0335	120	6.58	M07-02	2.55	0.071	0.0135	115	2.78
M03-02	6.41	0.083	0.0316	112	6.68	M07-03	2.75	0.134	0.0170	127	3.18
M03-03	5.76	0.098	0.0330	129	6.07	M07-04	3.07	0.246	0.0205	126	3.86
M03-04	6.19	0.070	0.0312	115	6.41	M07-05	2.79	0.233	0.0173	116	3.54
M03-05	5.73	0.081	0.0331	131	5.99	M07-06	2.77	0.174	0.0174	123	3.33
M03-06	6.09	0.079	0.0340	127	6.34	M07-07	3.16	0.262	0.0203	120	4.00
M03-07	6.10	0.073	0.0322	120	6.33	M07-08	3.03	0.254	0.0191	117	3.85
M03-08	4.82	0.073	0.0255	119	5.05	M07-09	2.49	0.069	0.0127	111	2.71
M03-09	4.85	0.080	0.0271	125	5.11	M08-01	2.54	0.234	0.0177	127	3.29

Table 1. (continued).

Grain No.	ThO_2 (wt%)	UO_2 (wt%)	PbO (wt%)	Age (Ma)	ThO_2* (wt%)	Grain No.	ThO_2 (wt%)	UO_2 (wt%)	PbO (wt%)	Age (Ma)	ThO_2* (wt%)
M08-02	2.41	0.067	0.0138	124	2.63	M14-03	6.10	0.789	0.0431	118	8.63
M08-03	2.61	0.071	0.0151	126	2.84	M14-04	5.92	0.712	0.0408	118	8.20
M08-04	3.19	0.080	0.0158	108	3.45	M14-05	6.11	1.08	0.0504	124	9.58
M08-05	2.68	0.069	0.0162	132	2.90	M14-06	6.16	0.655	0.0435	124	8.26
M09-01	4.34	0.067	0.0230	119	4.55	M14-07	5.86	0.681	0.0403	119	8.05
M09-02	5.79	0.082	0.0339	132	6.05	M14-08	6.43	1.14	0.0496	116	10.1
M09-03	6.74	0.079	0.0355	120	6.99	M14-09	6.89	0.651	0.0443	117	8.98
M09-04	7.11	0.100	0.0413	131	7.43	M14-10	5.72	1.04	0.0473	123	9.06
M10-01	6.65	0.857	0.0471	118	9.40	M14-11	6.06	0.889	0.0426	113	8.91
M10-02	6.35	0.629	0.0427	121	8.37	M14-12	6.20	0.854	0.0451	119	8.94
M10-03	6.28	0.661	0.0431	121	8.40	M14-13	6.49	0.717	0.0445	120	8.79
M10-04	6.87	0.536	0.0416	114	8.59	M14-14	6.46	0.808	0.0447	117	9.05
M10-05	6.47	0.726	0.0447	120	8.80	M14-15	6.26	0.236	0.0359	121	7.02
M10-06	6.55	0.598	0.0417	116	8.47	M14-16	6.80	0.723	0.0451	117	9.12
M10-07	6.46	0.840	0.0478	123	9.16	M14-17	7.51	0.355	0.0427	117	8.65
M11-01	5.66	0.088	0.0295	117	5.94	M15-01	11.8	0.230	0.0629	118	12.5
M11-02	8.88	0.181	0.0480	120	9.46	M15-02	7.73	0.150	0.0399	115	8.21
M11-03	7.26	0.136	0.0377	116	7.70	M15-03	10.7	0.207	0.0564	117	11.4
M11-04	7.97	0.165	0.0421	117	8.50	M15-04	15.0	0.270	0.0787	117	15.9
M11-05	5.93	0.094	0.0306	116	6.23	M15-05	11.5	0.191	0.0628	122	12.1
M11-06	8.30	0.163	0.0452	121	8.82	M15-06	7.75	0.125	0.0411	119	8.15
M12-01	6.43	0.098	0.0333	117	6.75	M15-07	8.16	0.112	0.0408	113	8.52
M12-02	6.11	0.076	0.0325	121	6.36	M15-08	11.1	0.189	0.0585	118	11.7
M12-03	5.78	0.095	0.0315	123	6.09	M15-09	12.9	0.219	0.0671	117	13.6
M12-04	5.70	0.105	0.0289	113	6.04	M15-10	6.50	0.132	0.0341	116	6.92
M12-05	6.02	0.110	0.0316	117	6.37	M16-01	6.36	0.124	0.0347	121	6.76
M12-06	4.96	0.101	0.0265	119	5.28	M16-02	6.68	0.331	0.0396	121	7.74
M12-07	5.56	0.100	0.0301	121	5.88	M16-03	6.33	0.100	0.0328	117	6.65
M12-08	6.56	0.120	0.0344	117	6.94	M16-04	9.98	0.158	0.0519	117	10.5
M13-01	8.97	0.115	0.0479	121	9.34	M16-05	6.39	0.103	0.0346	122	6.72
M13-02	3.77	0.092	0.0205	119	4.06	M16-06	6.25	0.112	0.0321	115	6.61
M13-03	3.68	0.117	0.0199	116	4.06	M16-07	6.03	0.102	0.0309	115	6.36
M13-04	3.97	0.080	0.0214	120	4.23	M17-01	4.36	0.099	0.0252	127	4.68
M13-05	5.67	0.189	0.0300	113	6.28	M17-02	4.46	0.080	0.0231	116	4.72
M13-06	5.86	0.189	0.0325	119	6.47	M17-03	4.33	0.074	0.0233	121	4.57
M13-07	5.94	0.143	0.0319	118	6.40	M17-04	4.36	0.093	0.0244	124	4.66
M13-08	6.60	0.141	0.0356	119	7.05	M17-05	4.48	0.084	0.0240	120	4.75
M13-09	10.2	0.136	0.0536	119	10.6	M17-06	4.50	0.074	0.0224	112	4.74
M14-01	6.53	0.762	0.0456	120	8.98	M17-07	4.35	0.084	0.0237	121	4.62
M14-02	6.52	1.06	0.0491	117	9.92						

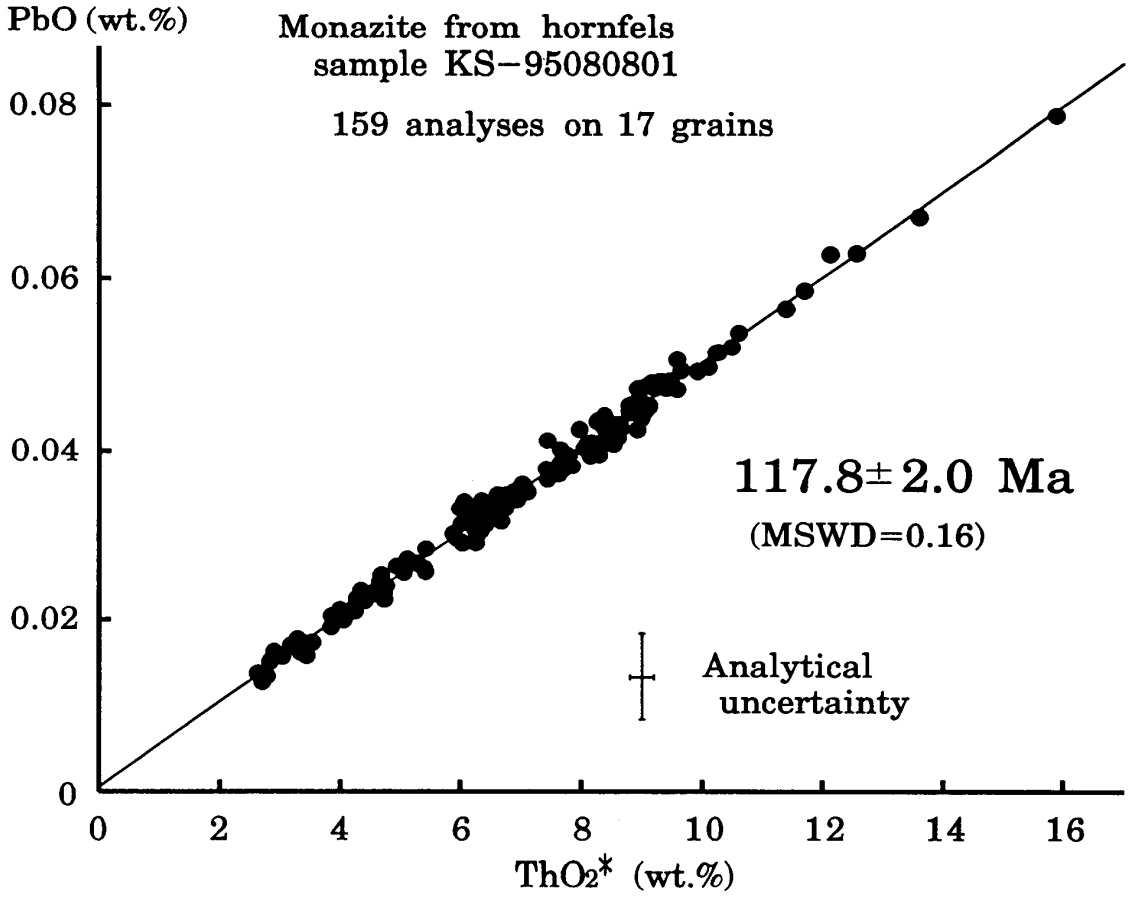

Fig. 3. Plots of PbO vs. ThO_2* for monazite grains from hornfels sample KS-95080801 in contact with the Kurihashi Granodiorite. Error bars in the figure represent 2σ analytical uncertainty, and the error given to the age is of 2σ.

from the Tono Granodiorite; they are 0.275 $^{87}Rb/^{86}Sr$ and 0.7047 $^{87}Sr/^{86}Sr$ for sample 70K-47, 0.374 $^{87}Rb/^{86}Sr$ and 0.7050 $^{87}Sr/^{86}Sr$ for sample 70K-49, 0.820 $^{87}Rb/^{86}Sr$ and 0.7058 $^{87}Sr/^{86}Sr$ for sample 70K-79, and 0.9411 $^{87}Rb/^{86}Sr$ and 0.7057 $^{87}Sr/^{86}Sr$ for sample 72K-569A. These data yield an isochron of 111.5 ± 40.4 Ma (MSWD = 0.02) with an initial $^{87}Sr/^{86}Sr$ ratio of 0.7043 ± 0.0004. The large error in the Rb-Sr whole-rock isochron age is evidently due to low Rb/Sr ratios of the Tono Granodiorite.

Although the 117.7 ± 2.0 Ma CHIME monazite age is slightly younger than the K-Ar biotite ages of 120, 120 and 122 Ma for the Kurihashi Granodiorite, the CHIME monazite and K-Ar biotite ages seem to be nearly identical within errors. This may simply mean that both the Th-U-Pb system in monazite and the K-Ar system in biotite were closed nearly at the same time. Since the K-Ar biotite age dates cooling to 300 ± 50°C (Berger and York, 1981; Harrison et al., 1985), the age relation suggests a rapid cooling of the Kurihashi Granodiorite subsequent to its emplacement.

The present study demonstrates the utility of the CHIME method for dating the emplacement age of monazite-free young granitoids. This is presumably of

use for any geochronological study of granitoids that are hardly dated through conventional isotopic methods owing to the presence of crustal contamination and inheritance, the absence of compositional variation required for isochron method, the inter-pluton thermal overprint and the intense weathering.

ACKNOWLEDGEMENTS

We would like to express our thanks to Dr. Y. Yusa, Mr. S. Yamasaki and Mr. K. Aoki of Power Reactor and Nuclear Fuel Development Corporation for their constructive comments. Our thanks are extended to Dr. K. Shibata and an anonymous reviewer for their thoughtful review of the manuscript. This work was in part supported by Grant-in-Aid for Fundamental Scientific Research (No. 07640656) from the Ministry of Education, Science and Culture, Japan.

REFERENCES

Adachi, M. and Suzuki, K. (1992) A preliminary note on the age of detrital monazites and zircons from sandstones in the Upper Triassic Nabae Group, Maizuru terrane. *Mem. Geol. Soc. Japan*, **38**, 111–120.

Berger, G.W. and York, D. (1981) Geothermometry from $^{40}Ar/^{39}Ar$ dating experiments. *Geochim. Cosmochim. Acta*, **45**, 795–811.

Corfu, F. and Muir, T.L. (1989) The Hemlo-Heron Bay greenstone belt and Hemlo Au-Mo deposit, Superior Province, Ontario. *Chem. Geol. (Isotope Section)*, **79**, 201–223.

Hamabe, S. and Yano, T. (1976) Geological structure of the Kamaishi mining district, Iwate Prefecture, Japan. *Mining Geol.*, **26**, 93–104.

Harrison, T.M., Duncan, I. and McDougall, I. (1985) Diffusion of ^{40}Ar in biotite: Temperature, pressure and compositional effects. *Geochim. Cosmochim. Acta*, **49**, 2461–2468.

Kano, H. and Research Group of Granite Plutons, Akita University (1978) Structural petrology of granite plutons, (1) the drop-form plutons in the Kitakami Mountainlands, Japan. *J. Japan. Assoc. Min. Pet. Econ. Geol.*, **73**, 97–120.

Kawano, Y. and Ueda, Y. (1965) K-A dating of igneous rocks in Japan (II) – Granitic rocks in Kitakami Massif –. *Sci. Rep. Tohoku Univ.*, Ser III, **9**, 199–215.

Nakai, Y. and Suzuki, K. (1996) CHIME monazite ages of the Kamihara Tonalite and the Tenryukyo Granodiorite in the eastern Ryoke belt of central Japan. *Jour. Geol. Soc. Japan*, **102**, 431–439.

Owa, E. (1950) Tsuchibuchi, *Quadrangle Series, Scale 1:50,000*, Geol. Surv. Japan.

Sawka, W.N., Banfield, J.F. and Chappell, B.W. (1986) A weathering-related origin of widespread monazite in S-type granites. *Geochim. Cosmochim. Acta*, **50**, 171–175.

Schärer, U., Hamet, J. and Allegre, C.J. (1984) The Transhimalaya (Gangdese) plutonism in the Ladakh region: a U-Pb and Rb-Sr study. *Earth Planet. Sci. Lett.*, **67**, 327–339.

Shibata, K. (1974) Rb-Sr geochronology of the Hikami granite, Kitakami mountains, Japan. *Geochem. J.*, **8**, 193–207.

Smith, H.A. and Barreiro, B. (1990) Monazite U-Pb dating of staurolite grade metamorphism in pelitic schist. *Contrib. Mineral. Petrol.*, **105**, 602–615.

Suzuki, K. and Adachi, M. (1991a) Precambrian provenance and Silurian metamorphism of the Tsubonosawa paragneiss in the South Kitakami terrane, Northeast Japan, revealed by the chemical Th-U-total Pb isochron ages of monazite, zircon and xenotime. *Geochem. J.*, **25**, 357–376.

Suzuki, K. and Adachi, M. (1991b) The chemical Th-U-total Pb isochron ages of zircon and monazite from the Gray Granite of the Hida Terrane, Japan. *J. Earth Sci., Nagoya Univ.*, **38**, 11–37.

Suzuki, K. and Adachi, M. (1994) Middle Precambrian detrital monazite and zircon from the Hida gneiss on Oki-Dogo Island, Japan: their origin and implications for the correlation of basement gneiss of Southwest Japan and Korea. *Tectonophysics* **235**, 277–292.

Suzuki, K., Adachi, M. and Kajizuka, I. (1994) Electron microprobe observations of Pb diffusion in metamorphosed detrital monazites. *Earth Planet. Sci. Lett.*, **128**, 391–405.

Suzuki, K., Adachi, M. and Nureki, T. (1996) CHIME age dating of monazites from metamorphic rocks and granitic rocks of the Ryoke belt in the Iwakuni area, Southwest Japan. *Island Arc*, **5**, 43–55.

Suzuki, K., Adachi, M. and Tanaka, T. (1991) Middle Precambrian provenance of Jurassic sandstone in the Mino Terrane, central Japan: Th-U-total Pb evidence from an electron microprobe monazite study. *Sediment. Geol.* **75**, 141–147.

Yoshida, T., Ozawa, A. and Katada, M. (1984) Morioka, *Scale 1:200,000 geological map*, Geol. Surv. Japan.

Yamazaki, H., Awata, Y. Shimokawa, K. and Kinugasa, Y. (1983) Akita, *Scale 1:500,000 Neotectonic Map Sheet 6*, Geol. Surv. Japan.